



Modeling and systematic investigation of a small-scale propeller selection

Original
Article

Mohammed Etewa¹, Ehab Safwat², Mohammed Abozied Hassan Abozied³,
Mohamed Misbah El-Khatib⁴

^{1,2,3}Guidance Department, ⁴Department of Electronic Engineering, Military Technical College, Cairo, Egypt

Keywords:

Blade element theory, flow simulation, Propeller model.

Corresponding Author:

Mohammed Etewa, Guidance Department, Military Technical College, Cairo, Egypt, Tel: +201006381777, Email: mohammed.etewa86@gmail.com

Abstract

The propulsion system has a dramatic effect on Unmanned Aircraft vehicles (UAVs) performance in addition to the indispensable function in creating a nonlinear flight simulation model for UAVs. Motivated by the problem of propeller modeling and selecting the highly appropriate propeller with affordable low computational time and power, this research focuses on carrying out a complete propeller performance assessment environment based on Enhanced Blade Element Theory (EBET). Contrary to the classical blade element theory (BET), the EBET considers the existence of the propeller angle of attack, as well as the free-stream velocity consequently accurate prediction of the aerodynamic loads furthermore The BET is reliable in moderate loading conditions and for reduced complexity geometries. In this regard, the APC 12X6E propeller is geometrically modeled based on digital scanning and manufacturer data furthermore operating conditions in the flight regimes. The propeller's static and dynamic performance characteristics are estimated to be used in UAV open-loop flight simulation model and to calculate the power coefficient. The assessment results show the efficiency of the proposed propeller simulated model..

I. INTRODUCTION

The growing number of designed small UAVs takes place due to their civilian and military ample field applications for instance survey, field surveillance, and protecting human life in several hazardous locations. Therefore, the UAVs entice the researcher's concentration accordingly to the numerous kinds of the UAVs design. The UAVs open-loop flight simulation model is increasingly important for performance analysis and design of a flight control system. The open loop flight simulation model accuracy is composed of the underlying five sub-models: atmospheric model, aerodynamic model, dynamics model, actuator model, and propulsion model. Propeller-driven is favored for small-scale UAVs since they are plentiful and affordable while still serving their purpose^[1,2,3]. The characteristics of the propeller are extremely important for engine and propeller compatibility achieving highly efficient propulsion during cruise flight with less efficiency importance in the rest of the flight phases (takeoff, climb, Descent, and landing) introducing multipoint optimization of the propeller selection. The foundation of the optimization process by developing numerical tools with low computational time.

W. J. MACQUORN^[4]carried out a significant advance in the theory of propellerthrough an investigation of marine propellers followed by Drzewiecki^[5]who introduced the blade element idea however each element would be affected by the propeller-induced velocity is not considered.

E. Eugene Larrabee^[6] proposed an applicable design theory for propellers with the least amount of induced loss after analyzing the steady air loads on the propeller. This approach combines vortex theory, momentum theory, and blade element theory.

Recently, several codes are currently available to design and estimate propellerperformance. These algorithms typically combine two-dimensional airfoil data with (BEM) however, codes that are appropriate for low Reynolds such as XROTOR (Drela and Youngren)^[7], QMIL (Drela)^[8], QPROP (Drela)^[9], and JAVAPROP (Hepperle)^[10,11].

This research introduces an applicable model for the propeller of an electrically propelled UAV. It aims to bridge the gap between the time-consuming CFD (computational fluid dynamics) which needs high computational resources^[12], and the propeller models based on expensive experimental wind tunnel testing. An effort was made to Develop an efficient procedure for estimating

the propeller performance. In addition, the propeller selection optimization exploits the efficiency prediction which is beneficial for the UAV's design phase. These are achieved through the incorporation of the propeller-

extracted geometric information extracted from propeller scanner software^[13] and the performance analysis software Javaprop^[11].

Nomenclature	
C	Chord length
S	Total blade area
α	Angle of attack
V	Local velocity vector
V_θ	Angular velocity
V_{ax}	Axial velocity
θ	Incidence angle
φ	Inflow angle
ΔT	Thrust produced by the element
ΔL	Lift produced by the element
ΔD	Drag produced by the element
ΔQ	Torque produced by the element
ΔF_θ	Circumferential force produced by the element
r	Distance between the current element and the rotational axis.
dr	Element section width.
C_l	Lift coefficient.
C_d	Drag coefficient.
ρ	Density of air.
C_t	Thrust coefficient
C_Q	Torque coefficient
J	Advance ratio
P	Propeller power consumption
η	Propeller efficiency
a	Axial inflow factor
a'	Tangential inflow factor

This paper is organized as follows; section 2 presents the detailed mathematical modeling of the propeller. The propeller simulated results and the proposed propeller model are highlighted in section 3. Finally, the study is concluded in section 4.

2- Analysis of the proposed methodology

2.1 Blade Element Momentum Theory (BET)

BET is one of the theories used to estimate the propeller's aerodynamic loads^[1]. BEM uses the geometry of the propeller blades, including the airfoil geometric data and chord, as well as the local incidence angle at each section. It calculates the thrust and torque at an arbitrary radial location along the blade. The blade is divided into elementary portions. It is assumed that there are no aerodynamic interactions between the various blade when the circumferential distance between the blades and the blade chord is sufficiently high:

$$\frac{s}{c} \gg 1 \quad (1)$$

However, for this reason, it is valid only for a small number of blades. Additionally, just the two-dimensional lift and drag statistics of the blade element airfoil are used to calculate thrust and torque on the blade elements in accordance with the local angle of attack α in the presence of the free stream velocity. The local velocity vector for each section V is the summation of angular velocity V_θ and the axial velocity V_{ax} . This local velocity V vector creates α with the propeller chord. Each section is set at a certain given geometric incidence angle θ as represented in Fig.1. The difference in angle between the lift and thrust vector is φ

$$\varphi = \theta - \alpha \quad (2)$$

$$\varphi = \tan^{-1} \left(\frac{V_{ax}}{V_\theta} \right) \quad (3)$$

Using basic trigonometry, we can write that the elemental thrust and circumferential force are respectively

$$\Delta T = \Delta L \times \cos\phi - \Delta D \times \sin\phi \quad (4)$$

$$\Delta F_{\theta} = \Delta D \times \cos\phi + \Delta L \times \sin\phi \quad (5)$$

The torque required to turn that element of the blade is:

$$\Delta Q = r \times \Delta F_{\theta} \quad (6)$$

$$\Delta L = 0.5 C_l \rho V^2 \times C \times dr \quad (7)$$

The Drag force for each element is:

$$\Delta D = 0.5 C_d \rho V^2 \times C \times dr \quad (8)$$

Where C_p and C_d are the lift and drag coefficients corresponding to (α) , Consequently, thrust and torque equations for B blades:

$$\Delta T = 0.5 \rho V^2 \times (C_l \times \cos\phi - C_d \times \sin\phi) B \times C \times dr \quad (9)$$

$$\Delta Q = 0.5 \rho V^2 \times (C_l \times \sin\phi + C_d \times \cos\phi) B \times C \times dr \times r \quad (10)$$

The total thrust of the propeller is calculated from:

$$T = \sum_1^j \Delta T \quad (11)$$

Where (j) number of element sections.

Similarly, the total torque of the propeller is calculated.

$$Q = \sum_1^j \Delta Q \quad (12)$$

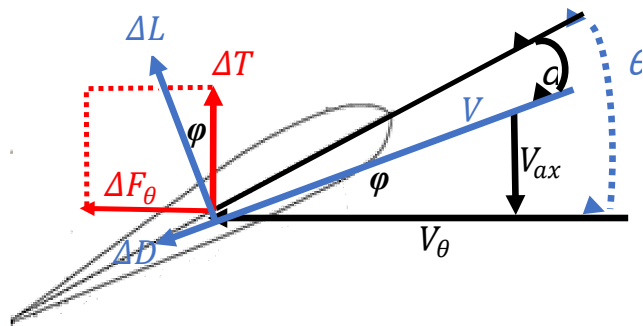


Fig. 1: Forces acting on a blade section

Thrust and torque coefficients are calculated as follows:

$$C_t = \frac{T}{\rho n^2 D^4} \quad (13)$$

$$C_Q = \frac{T}{\rho n^2 D^5} \quad (14)$$

In the dynamic mode, the efficiency is estimated at different values of advance ratio (J), which is calculated as:

$$J = \frac{V}{nD} \quad (15)$$

$$\eta = \frac{TV}{P} = \frac{C_t}{C_p} J \quad (16)$$

If the chord length and incidence angle along the blade is defined. they can be used directly. However, if the detailed geometry is not available it could be estimated. EBET based on the blade element theory, able to determine the extra axial and circumferential velocity that each blade segment adds to the entering flow. This increased speed produces anspeeding up the flow and consequently the thrust. When the propeller's power and thrust loading (power per disc area) is low, this basic model typically performs admirably. The mathematics described in "Design of Optimum Propellers by C N Adkins", Where:

$$\phi = \tan^{-1} \left(\frac{V_{ax}(1+a)}{V_{\theta}(1-a')} \right) \quad (17)$$

In the process of predicting the propeller geometrical data could be obtained physically by cutting the propeller into fixed-width sections as shown in Fig.2[1]. On the contrary, the proposed solution in this research the tested propeller is APC 12X6E shown in Fig.3 where geometry data for the propellers is estimated using 'Propeller Scanner'^[13]. This software tries to rebuild the propeller blades' shape from digital photographs. This method yields the propeller chord, twist, and pitch distribution along the blade radius. In addition ,to identify the twist angle and the chord at any section from the digital photo, the distance C in Fig.3 is measured from the projection of the chord on the rotation plane top view, where:

$$\bar{C} = C \cos\theta \quad (18)$$

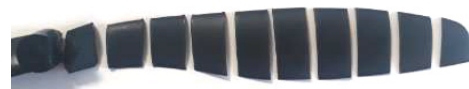


Fig. 2: Obtaining the propeller Geometry by cutting^[1]

The projection of the chord length in the plane normal to rotation plane shown in Fig.3 front view marked as Δx where:

$$\Delta x = C \sin\theta \quad (19)$$



Fig. 3: APC 12X6E Propeller top and front views

From (18) and (19), The twist angle at distance dr is:

$$\theta = \tan^{-1} \frac{\Delta x}{\bar{c}} \quad (20)$$

Thus, the propeller chord and twist distribution along the blade radius are identified and presented in Fig.4

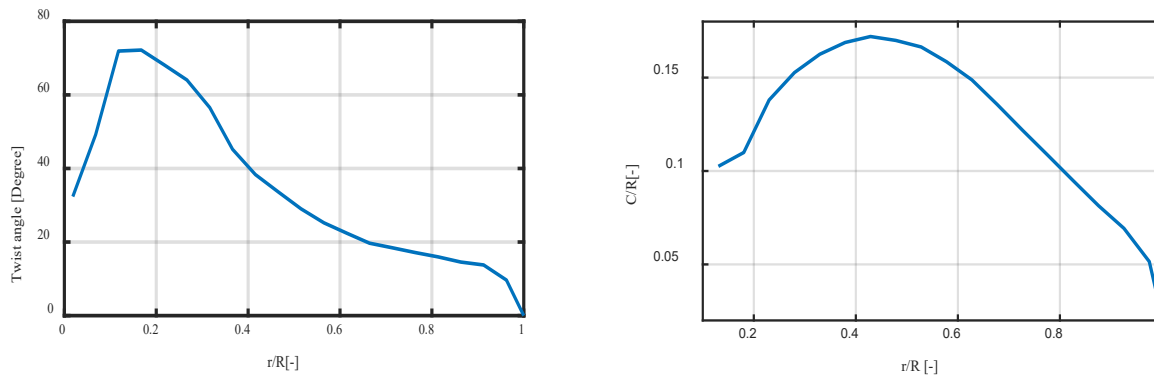


Fig. 4: Chord and twist distribution

The implementation of BET coupling with two-dimensional airfoil characteristics is considered in a cost-efficient simulation. It is met in the JAVAPROP environment with a graphical user interface (GUI). It uses the input parameters of an existing propeller to calculate the performance. The off-design data and flight conditions such as "number of blades, rotating speed, propeller diameter, spinner hub diameter, the air density, and UAV velocity V " are provided furthermore the propeller divided sections. This is done according to BET which is extracted from the digital photo. After that, they entered three fields the section radius, the section chord, and the twist angle to calculate the thrust and torque at an arbitrary radial section along the blade. Java Prop divided the provided propeller geometrical data into four airfoil sectors and interpolates between these sectors to calculate the final thrust and torque as represented in Fig. 5. The generated propeller model based on the equations described in the previous sections is compared with manufacturer data^[14].

For the comparison thus the static thrust, and torque obtained and plotted versus the propeller rotational speed RPM in Fig.6 to show the comparisons of the static thrust and torque obtained from classical BET, EBET, and the manufacturer-published data and the result show that the BET and EBET represent good estimation result up to 6000 [RPM] after that the axial and tangential inflow factors that considered in the EBET expressed better estimation performance than the classical BET. In addition, thrust and power coefficients are calculated according to equations (13,14) and plotted versus the advance ratio J as represented in Fig.9 for the dynamic simulation, a study of the effect of UAV velocity starting from static until the propeller reaches the windmill. The propeller characteristics were presented and the efficiency is plotted versus the advance ratio J to estimate the most efficient advance ratio towards the propeller selection process^[15]. Finally, the flow field demonstrates the flow through the propeller including the contraction of the stream tube as well as the swirl losses.

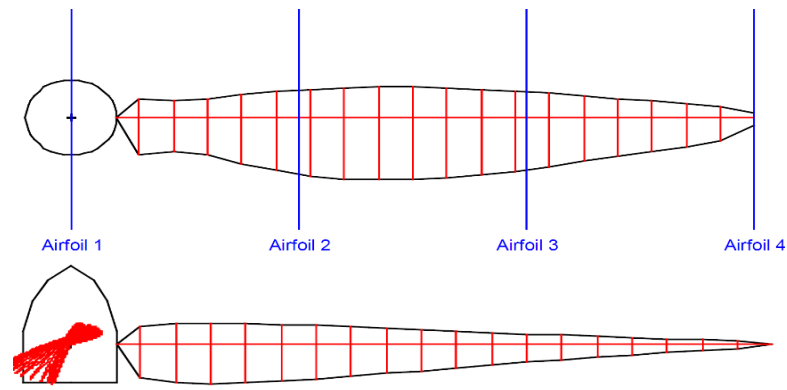


Fig. 5: Top and front view of propeller sections

3-The simulation Results

3.1 Propeller Static Performance Simulation Results

The results of the static performance are demonstrated in the quadratic form for torque, thrust and, power shown in Fig.6, and Fig.7 as a function of RPM for modeling

purposes. Static performance data over the simulated range of RPM is a good judgment and easy to use the proposed thrust mathematical model in the flight simulation model and the counterpart torque and power required to be delivered by the motor.

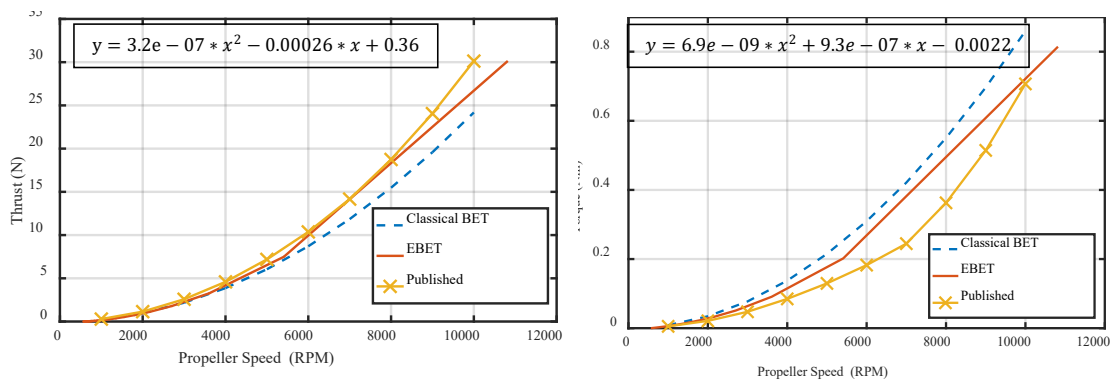


Fig. 6: Static thrust and torque comparison

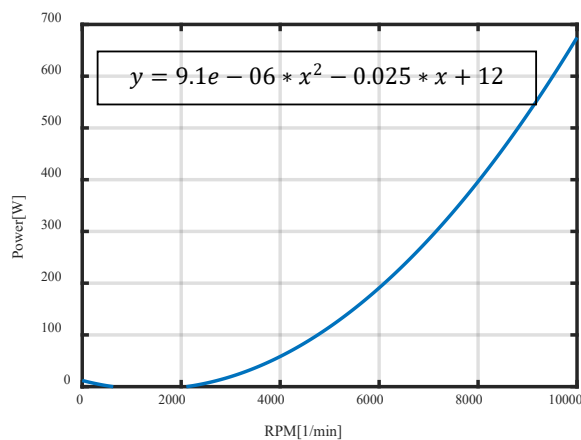


Fig. 7: Static power consumption

3.2. The results of the Propeller Dynamic Performance

The dynamic performance data is presented as a function of the free stream velocity at 9000 RPM used as a selective result to demonstrate the thrust and torque dynamic performance.

The proposed mathematical model is characterized by a polynomial fitting as shown in Fig. 9. It is evident that the thrust curve vicissitudes from positive to negative around $V=32[m/s]$, which determines the beginning of the braking mode region at $V>32[m/s]$. In addition, the torque curve shows that the torque changes from positive to negative at

nearly $V=34[m/s]$. the region of the windmill is defined for $V>34[m/s]$, From the efficiency curve in Fig.10. It can be found that the maximum efficiency equals approximately (0.62) at J near (0.45). Moreover, it is noticeable that the efficiency is zero means the thrust goes negative. The airflows of the simulated propeller model are demonstrated in Fig.11. It illustrates the axial velocity ratio before and after the propeller in form of a contour plot including the contraction of the stream tube. The test results designate that the objectives are achieved without wind-tunnel tests or computational fluid dynamics for selected propellers are also presented.

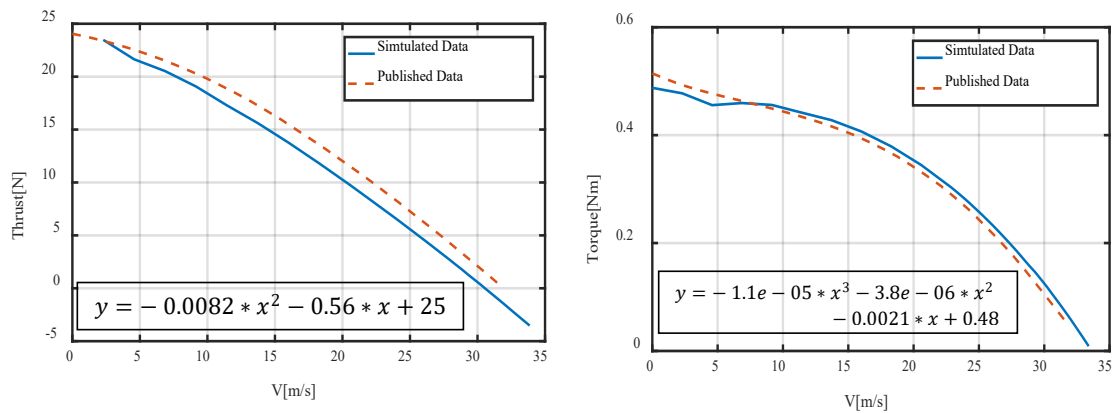


Fig. 8: Dynamic thrust and torque

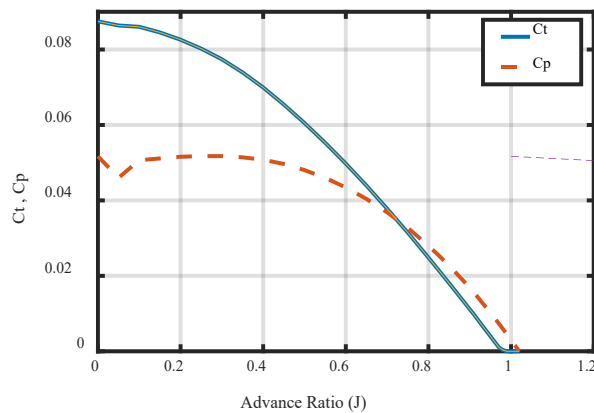


Fig. 9: Thrust and power coefficients

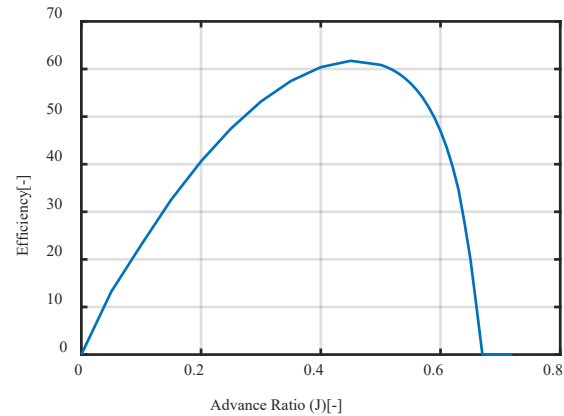


Fig. 10: Propeller dynamic efficiency

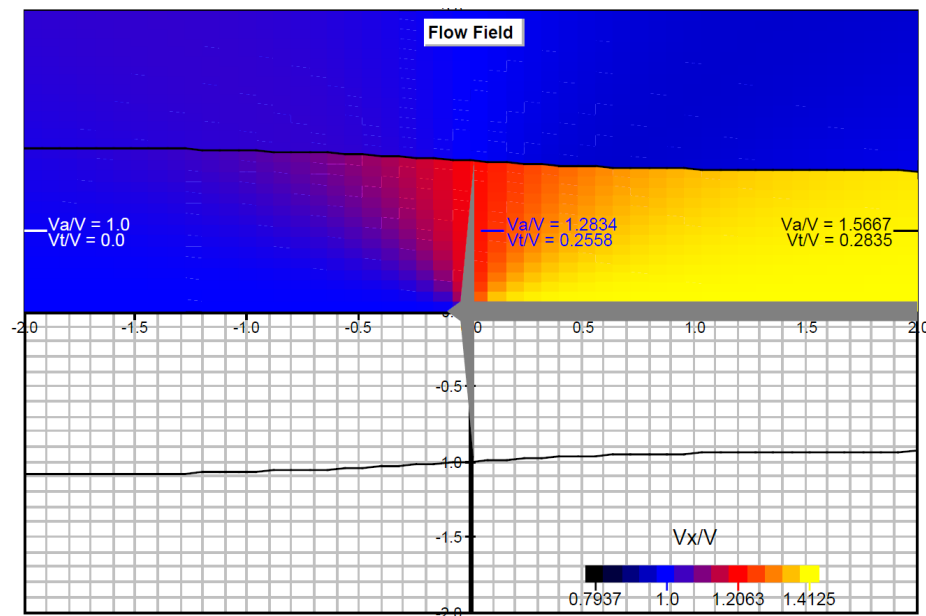


Fig. 11: Axial velocity of the flow in the Simulation model

5. Conclusion

This paper proposed a simplified method for propeller modeling with different operating conditions based on EBET. Static and dynamic performance of thrust, torque, and power prediction capabilities are obtained with acceptable accuracy in the absence of detailed geometric data. Simply extract the propeller geometrical data in contrast to the distribution of chord length and blade twist angle data using top and side view digital images. The result is affordable and faster than CFD, the real flight test, and the wind tunnel. Facilitate propeller selection based on propeller geometry and operating condition with maximum efficiency during an optimization procedure. The advantages of the propeller simulation tool JavaProp is verified as fast and provide some primary data, which could be used as an initial guess of power and thrust versus advance ratio for the propeller preliminary design.

6. References

- [1] D. Kaya, "Estimation of Aerodynamic Loads of a Propeller through Improved Blade Element and Momentum Theory and Propeller Design Optimization." <https://www.researchgate.net/publication/353923745>
- [2] D. Kaya, A. Kutay, and H. Özkanaktı, "Flight Time Calculation of a Blended-Wing-Body UAV through Improved Blade Element and Momentum Theory," Oct. 2021.

- [3] J. B. Brandt and M. S. Selig, "Propeller Performance Data at Low Reynolds Numbers," 2011. <http://www.ac.illinois.edu/m-selig>
- [4] J. Morgado, M. A. R. Silvestre, and J. C. Páscoa, "Validation of new formulations for propeller analysis," in *Journal of Propulsion and Power*, Jan. 2015, vol. 31, no. 1, pp. 467–477. doi: 10.2514/1.B35240.
- [5] S. Drzewiecki, *Méthode pour la détermination des éléments mécaniques des propulseurs hélicoïdaux*. imprimerie Gauthier-Villars et Fils, 1892.
- [6] E. E. Larrabee, "Practical design of minimum induced loss propellers," *SAE Transactions*, pp. 2053–2062, 1979.
- [7] M. Drele and H. Youngren, "Axisymmetric analysis and design of ducted rotors," *DFDC software manual*, 2005.
- [8] M. Drele, "QMIL user guide," *Propeller Analysis and Design URL*: <http://web.mit.edu/drele/Public/web/qprop>, 2005.
- [9] M. Drele, "QPROP formulation," *Massachusetts Inst. of Technology Aeronautics and Astronautics*, Cambridge, MA, 2006.
- [10] M. Hepperle, "Inverse aerodynamic design procedure for propellers having a prescribed chord-length distribution," *J Aircr.*, vol. 47, no. 6, pp. 1867–1872, 2010.
- [11] M. Hepperle, "JavaProp Users Guide.", 2010.
- [12] O. Bergmann, F. Götten, C. Braun, and F. Janser, "Comparison and evaluation of blade element methods against RANS simulations and test data," *CEAS Aeronaut J.*, vol. 13, no. 2, pp. 535–557, Apr. 2022, doi: 10.1007/s13272-022-00579-1.
- [13] M. Hepperle, "PropellerScanner Manual," <http://www.mh-aerotoools.de>, 2003.
- [14] APC Propeller, "APC 12X6E /technical-information/performance-data/," https://www.apcprop.com/files/PER3_12x6E.dat.
- [15] A. M. Kamal, A. M. Bayoumy, and A. M. Elshabka, "Modeling and simulation of propeller propulsion model using wind tunnel," in *AIAA Modeling and Simulation Technologies Conference*, 2015, 2015. doi: 10.2514/6.2015-1596.